Original Research

Evaluation methods of a rat sciatic nerve crush injury model

Yun An[1],*,[†], Hui-Xin Yan[1],[†], Jiang-Na Zhao[1],[†], Xu-Ming Yang[2], Jun-Tao Yan[1],*

[1]Department of Tuina, Yueyang Hospital of Integrated Traditional Chinese and Western Medicine, Shanghai University of Traditional Chinese Medicine, 200437 Shanghai, China

[2]Acupuncture and Tuina College, Shanghai University of Traditional Chinese Medicine, 201023 Shanghai, China

*Correspondence: yanjuntao@shutcm.edu.cn (Jun-Tao Yan); anyun@shutcm.edu.cn (Yun An)

[†]These authors contributed equally.

Abstract

Background: The rat sciatic nerve crush injury model is one of the most commonly used models to research peripheral nerve injury (PNI), however, the evaluation of the model preparation lacks exact standards. This study aimed to investigate accurately assessment methods for research concerning the rat sciatic nerve crush injury. **Methods**: The sciatic nerve crush injury model of was performed using the FST toothless forceps. The corresponding locations and pressures of different ratchet strengths were assessed by using CMAP, behavioral, and morphological methods. **Results**: In each group of PNI, motor and sensory functions were gradually restricted on the injured side of rats as the applied pressure increased. CMAP was more sensitive to nerve injury arising out of the force values obtained from the forceps. **Conclusions**: As a sensitive indicator for PNI, the neuroelectrophysiological examination was more likely to reflect the morphological changes of injured nerves. These findings may provide a standardized approach to sciatic crush injury modelling.

Keywords: Sciatic nerve crush injury; Neuroelectrophysiological

1. Introduction

Peripheral nerve injury (PNI), which disturbs behavioral function and reduces quality of life, has emerged as a major problem in rehabilitation medicine [1,2]. In contrast to the central nervous system, the peripheral nervous system exhibits a significant self-repair and regenerative capacity following peripheral nerve injury [3,4]. However, complex injuries with substantial loss of nerve tissue and a subsequent defect between the nerve ends often require therapeutic intervention for functional restoration. Currently, autologous nerve grafts harvested from another site in the body, are considered the best procedure for restoration of structural and functional nerve regeneration. Unfortunately, the effects of this treatment therapy for PNI is not completely satisfactory [5].

Nerve repair and regeneration are difficult to study *in vitro* [6], for this reason animal experiments are still preferred. The rat sciatic nerve crush injury has been considered the best model to study peripheral nerve regeneration and is most commonly used due to the widespread availability of rats as well as the distribution of their nerve trunks which is similar in humans [7,8]. It provides a nerve trunk with adequate length and space at the mid-thigh for surgical manipulation and allows investigators to apply a standard direct trauma in rats, cause a temporary or permanent change to its neurological function and ultimately results in a lesion similar to those seen in patients with PNI [9].

Mechanical techniques, such as toothless forceps, are the most frequently used tool for implementing the sciatic nerve crush injury model and provide an approach that may reduce operating time [10]. However, a possible limitation of the nerve crush model is that the number of nerve fibers suffering structural damage may vary considerably depending on different degrees of nerve compression, thus making the method unreliable. Indeed, some nerve fibers might undergo only a temporary functional impairment and the subsequent neurological functional recovery may not be due to a true regeneration of the severed axons [11]. Therefore, an accurate assessment of the PNI model remains a difficult task. For this reason, by a combination of both functional and morphological assessment, this study focused on the corresponding location and pressure of different rachet strengths using CMAP and behavioral and morphological methods, resulting in accurately assessment methods for research concerning the rat sciatic nerve crush injury.

2. Materials and methods

2.1 Animals

Total of 63 Sprague–Dawley (SD) male rats (180 ± 10 g) were obtained from the Shanghai Jihui Laboratory Animal Co., Ltd. (Shanghai, China). They were reared in separated cages in the Animal Center of the Affiliated Yueyang Hospital of Integrated Traditional Chinese and Western Medicine, Shanghai University of Traditional Chinese Medicine. The room was maintained at 18–21 °C and 40–50% humidity, with day-night cycle lighting (12 h–12 h). Rats were acclimated in the environment for one week prior to the experiment.

2.2 Animal model preparation and grouping

The sciatic nerve crush injury model of SD male rat was performed using the FST toothless forceps (model: 13006-12). Two positions were selected for crush application in the modeling. They were located at point 1/3 of the distance from the tip of the forceps to the hinge (~1.5 mm wide) and 1/3 of the distance from the hinge towards the tip of the forceps (~2.3 mm wide), and pressed separately 1 notch (the degree of crush was one tooth selected in the rachet in the handles), 2 notches (the degree of crush was two teeth selected in the rachet in the handles), and 3 notches (the degree of crush was three teeth selected in the rachet in the handles) at either of the different positions. Rats were randomly divided into seven equal groups of nine: normal control group, distal one notch group, distal two notches group, distal three notches group, proximal one notch group, proximal two notches group and proximal three notches group according to its location and quantitative notch number. The control group did not undergo surgery.

Rats were anesthetized with intraperitoneal injection of 2% pentobarbital (30 mg/kg) and the rat sciatic nerve crush injury model was prepared as reported [11–14]. In short, the skin of the lower left limb was prepared, and the rat was placed in the prone position. Under aseptic conditions, exposure of the left sciatic nerve was performed through an incision on the mid-high of the left hind limb. The FST non-serrated clamp was used for a period of 60 s to create a sciatic crush injury, 10 mm above the bifurcation, to obtain good reproducibility of the sciatic crush injury model. Marked with a 11–0 non-invasive suture, the sciatic nerve was then replaced. To minimize differences between animals, all surgical preparation was performed by the same person. Since the clamp position is the sciatic nerve trunk, care was taken to avoid injuring the bifurcation between the common peroneal and tibial nerves during the whole surgery.

2.3 Experimental design and procedure

Rats were tested by behavioral assays before surgery to establish baseline measures. Food intake, gait, incision and infection were observed after the operation and survivals were recorded. Rats of each group were sacrificed three days after surgery for electrophysiological evaluation and behavioral and morphological observation.

2.3.1 Electrophysiological examination

An electrophysiological examination was performed after behavioral assays on the third day following the operations in each group. Following anesthesia, rats were fixed and the left sciatic nerve was exposed for a length of about 2.0 cm. The compound muscle action potential (CMAP) was measured by a MEB-9404C type electrodiagnostic device (Hitachi Ltd., Tokyo, Japan). Disposable acupuncture needles were inserted into each of the muscle belly and the tendon. A recording needle electrode was inserted into the middle of the gastrocnemius, a reference needle electrode was inserted near the Achilles tendon and the ground electrode was placed on the tail. A bipolar hook electrode for electrical stimulation contacted the sciatic nerve distal and proximal to the injury sites. Latency and amplitude were measured and recorded with a stimulation time of 0.2 ms and single-pulse frequency of 1 Hz. Motor nerve conduction velocity (MNCV) was calculated from MNCV (m/s) = the distance between stimulating electrodes (m)/latency difference of action potential (s).

2.3.2 The sciatic functional index

Referring to reported methods [15], rats were tested in a confined walkway 60 cm long and 10 cm wide with a side wall height of 15 cm. The hind paws of rats were wet with ink and they walked on a strip of paper to record the paw prints. Footprints with clear imprints were selected to measure the following three variables: PL (the distances between the third toe and the heel), TS (distance from the first and the fifth toe), and IT (distance between the second and the fourth toe). The sciatic functional index (SFI) value was calculated by the method proposed by Bain *et al*. [16]. SFI = 109.5 (ETS – NTS)/ NTS – 38.3 (EPL – NPL)/NPL + 13.3 (EIT – NIT)/ NIT – 8.8; where "N" indicated the normal feet and "E" indicated the experimental feet. SFI values that approached –100 represent increasingly greater impairment, whereas SFI values closer to 0 imply increasingly normal motor function.

2.3.3 Determination of bipedal 50% mechanical PWT

Rats were tested for their paw withdrawal threshold (PWT) values for mechanical sensitivity using von Frey filaments (Stoelting Co., Ltd., Wood Dale, IL, USA) according to the up-and-down method [17,18]. Each rat was placed on an elevated transparent plexiglass box (20 cm $\times$ 10 cm $\times$ 20 cm), the bottom of which was a 10 mm $\times$ 10 mm wire mesh and allowed to adapt for 30 minutes. This test was conducted at a constant temperature in a noise-free room. When the rat had relaxed, a series of von Frey filaments (2 g, 4 g, 6 g, 8 g, 10 g, 15 g, 26 g) were then used to stimulate the center of the rat hind paw with a stimulating force that caused the filament to form a slight S-shape as the standard for full force. The stimulation time was no longer than 8 s and the interstimulus interval was at least 60 s. Starting from 10 g, flinching or licking the paw were defined as positive reactions and expressed as "X". The filament was then replaced with a neighboring filament of a lower level; if there was no response, the reaction was expressed as "O". A sequence was then obtained, with an "O" anterior to "X" assumed as the starting point. Six consecutive stimuli including the starting point were selected as key sequences to calculate the threshold of the 50% mechanical PWT. The computational formula for this was: 50% mechanical PWT $(g) = \left(10^{[Xf+\kappa\delta]}\right)/10000$, where Xf is the

Fig. 1. Representative CMAP recordings of the injured side at 3 days after surgery.

logarithmic value of the last von Frey filament in the sequence, δ is the logarithmic average difference of each filament intensity, which equaled approximately 0.192, and the k value was obtained by look-up table according to the measured "X" and "O" sequence.

2.3.4 Paw withdrawal latency

The Hargreaves method was used to assess the thermal hyperalgesia evoked paw withdrawal response [19]. Before the experiment, rats were placed in a transparent plexiglass box (20 cm × 10 cm × 20 cm), the bottom of which was an evenly heated glass platform (IITC Life Science Instruments Model 33, Woodland Hills, CA, USA). This test was conducted at a constant temperature in a noise-free room. In the quiet state, a radiant heat source was focused onto the plantar surface of the injured hind paw. The heat source was turned off when the rat withdrew the hind paw and the time from the start of the radiant heat application to the withdrawal of the paw was defined as the paw withdrawal latency (PWL) [20]. To prevent injury to the rat, the duration of each stimulus was set to 20 s. If the rat failed to respond within this time, the heat source was automatically switched off. The interval between the two tests of the same rat was not less than ten minutes and the average of the three measurements was expressed as the PWL of the rat.

2.3.5 Histological examination

After anesthesia, the nerve tissue was taken from the affected side and fixed with 4% paraformaldehyde. Subsequently, the tissues were dehydrated and embedded in paraffin and sliced into 5 μm sections. The Paraffin-embedded tissues were then dewaxed with xylene and alcohol and stained with hematoxylin-eosin (H&E). Finally, any histopathological changes were observed under an optical microscope.

2.4 Statistical analyses

These data were analyzed using GraphPad Prism7 (Manufacturer, La Jolla, CA, USA). Any significant differences were analyzed by using one-way ANOVA combined with an LSD t-test. All data are presented as means ± SD.

3. Results

3.1 Electrophysiological examinations

For CMAP amplitude, latency and NCV, an electromyogram evoked potential instrument was used for recording and calculation. The results suggested that for SNI modeling, CMAP was sensitive to nerve injury arising out of the force values obtained from the forceps (Fig. 1). The original data of CMAP for each group were illustrated in Table 1. The amplitude of sciatic nerve in control rats averaged 26.98 ± 4.66 mV. For each injury group, it was found that the distal three notches group showed a clear decrease in amplitude (47.70% of control; 14.11 ± 2.55 mV). The distal two notches group showed a greater decline close to 0 in amplitude (0.17 ± 0.29 mV). The amplitudes of the remaining injury groups were undetectable. It was found that the latency of sciatic nerve in normal rats was about 0.15 ± 0.03 ms, while the latency for the distal three notches group was approximately 0.29 ± 0.03 ms. The remaining groups could not be measured for latency due to the serious nerve injury caused by excess force values. The NCV of the control and distal three notches group were approximately 58.18 ± 8.55 m/s and 22.28 ± 3.27 m/s, respectively. As was the case with the latency, no NCV was measurable in the other injury groups.

3.2 SFI

SFI is a classic measure of the function of sciatic nerve, which directly reflects the motor function after PNI. All rats tested were measured and the value of SFI was calculated before modeling on the day of modeling and three days after modeling. Detailed results are presented in Fig. 2. On the day of modeling, analysis showed that there were significant differences for all injury groups compared to the control group ($p < 0.001$). Differences between the distal one notch group and the other groups were not statistically significant for SFI with the exception of the distal three notches group ($p < 0.01$). Three days after modeling, all injury groups showed significant differences compared to the control group ($p < 0.001$). In addition to the distal two notches group ($p < 0.01$), the distal three notches group (p

Table 1. Detailed data after crushing of the rat sciatic nerve.

Classification	Neuropathophysiology	Group	CMAP		
			Amplitude (mV)	Latency (ms)	NCV (m/s)
Normal	Nerve structure remains intact	Control	26.98 ± 4.66	0.15 ± 0.03	58.18 ± 8.55
Sunderland grade I	Segmental myelin damage, transient blockage in neural guidance, the elements of connected tissue (endoneurium, perineurium, epineurium) remains intact and axonal integrity is preserved, partial sensory-motor impairments	Distal three notches	14.11 ± 2.55	0.29 ± 0.03	22.28 ± 3.27
Sunderland grade II	Damage in axon and its surrounded myelin, nerve continuity and surrounding connecting tissues (endoneurium, perineurium, epineurium) are maintained, impairments in autonomic and sensory-motor functions	Distal two notches	0.17 ± 0.29	–	–
Sunderland grade III	Damage in axon, demyelination, endoneurium is disrupted but perineurium and epineurium are remained	Distal one notch / proximal one notch / proximal two notches	– / – / –	– / – / –	– / – / –
Sunderland grade IV	Axonal and myelin damage, endoneurium and perineurium are disrupted, epineurium is maintained	Proximal three notches	–	–	–
Sunderland grade V	Axonal and myelin damage, nerve continuity and surrounding connecting tissues (endoneurium, perineurium, epineurium) are disrupted	This grade of nerve injury cannot be achieved with FST toothless forceps.			

Data mean $\pm$ SD; – indicates undetectable CMAP level.

< 0.001) and the proximal three notches group ($p < 0.05$), no significant difference was observed between any other groups compared with the distal one notch group after pairwise comparisons ($p > 0.05$).
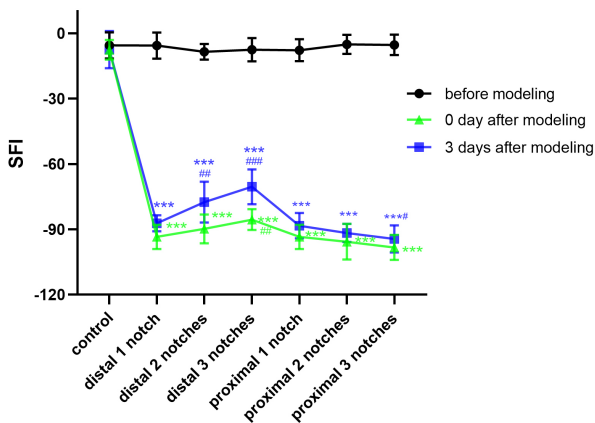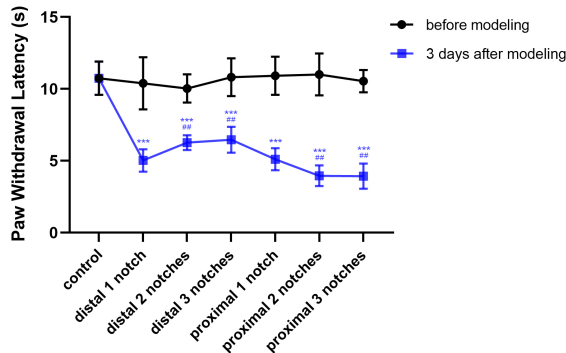

Fig. 2. Crush data compared with the control group (mean $\pm$ SD, n = 9; ***$p < 0.001$); compared with the distal 1 notch group (###$p < 0.001$, ##$p < 0.01$, #$p < 0.05$).

3.3 PWT

PWT is one of the major means by which to evaluate sensory function of peripheral nerves. The level of PWT was measured as 24.09 ± 6.73 g in normal rats and this value gradually decreased as the applied pressure increased. As shown in Fig. 3, the PWT in all injury groups were statistically significant when compared to the control group ($p < 0.001$). Compared to the distal one notch group, no statistically significant differences were found using the LSD t-test between all pairs, with the exception of the distal two and three notches groups ($p < 0.001$, $p < 0.001$).
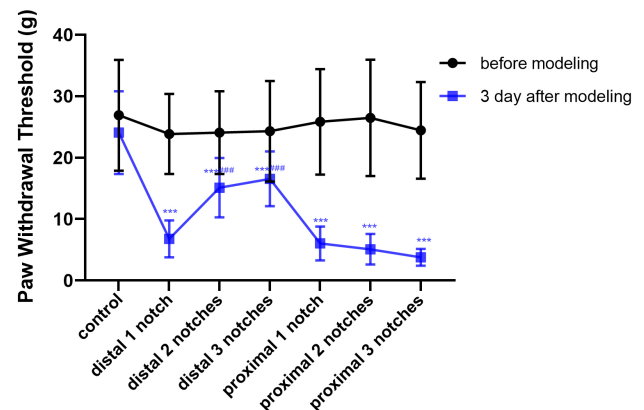
Fig. 3. Crush data compared with the control group (mean $\pm$ SD, n = 9; ***$p < 0.001$); compared with the distal 1 notch group (###$p < 0.001$).

3.4 PWL

The sensory function of peripheral nerve can be evaluated by measuring the PWL. It was found that the control PWL was about 10.75 ± 1.15 s, but that the PWL of sciatic nerve was significantly reduced after modeling (see Fig. 4). A significant difference was found when compared with the control group for the PWL ($p < 0.001$). And compare to the distal one notch group, there were significant differences between all pairs of groups other than the proximal one notch group ($p > 0.05$).

Fig. 4. Crush data compared with the control group (mean $\pm$ SD, n = 9; ***$p < 0.001$); compared with the distal 1 notch group (##$p < 0.01$).

3.5 Histological examination

Three days after crush, sciatic nerves cross- and longitudinal-sections acquired from the control and different injury groups were examined by microscopy using H&E staining and microscopy images (Fig. 5). Transverse sections through the sciatic nerve showed nerve fibers to display round-shaped structures of various sizes and axons were arranged closely with purple-red staining in the centre of myelinated nerve fiber bundles. The surrounding low-stained areas represented myelin. The deeply stained areas represented Schwann cells nuclei, which appeared between the myelinated fiber bundles. Endoneurium wrapped around the surface of each nerve fiber as a thin layer of connective tissue. Nerve fiber bundles were surrounded by perineurium, its outer layer comprised connective tissue, and the inner layer was multilayer flattened epithelial cells. The epineurium was a dense regular connective tissue which wrapped around the surface of nerve. Longitudinal section showed that the normal nerve was enveloped in this connective tissue. Myelinated nerve fibers presented with a neatly arranged wavy profile. Nodes of Ranvier, small numbers of red cells and Schwann cells nuclei were also visualized. The whole nerve structure appeared complete and was densely arranged.

The damage incurred by each injury group was observed in both cross- and longitudinal sections. It was found that the sciatic nerve in the distal three notches group was the least severely damaged and the overall sequence of nerve fibers was relatively dense. Nodes of Ranvier were seen between nerve fibers, some axons developed oedema, myelin were compressed, but all the connective tissues such as endoneurium, perineurium and epineurium were structurally intact. The sciatic nerve in the distal two notches group exhibited a lesser extent of damage. Its axons were broken with myelin destruction, but endoneurium, perineurium and epineurium appeared intact. Meanwhile, this strength of damage reduced nerve fiber compactness and they were loosely arranged. The distal one notch group showed a degree of injury comparable to the proximal one notch group. Both were observed to exhibit broken nerve fibers and were arranged in a chaotic way. Axons were broken and surrounded by myelin destruction and a small amount of inflammatory cell infiltration. Additionally, the endoneurium was partially impaired, but perineurium and epineurium presented intact. The proximal two notches group suffered from more severe damage. Different structural injury was revealed including broken nerve fibers, increasing axon dispersement, irregular arrangement, myelin breakdown with vacuolar degeneration and inflammatory cell infiltration. The endoneurium was bisected, but the perineurium and epineurium remained intact. Among these groups, the damage of the proximal three notches group was the most serious. Nerve fibers were broken and disordered, the broken axons were clearly swollen and the surrounding myelin was disintegrating and broken down with obvious inflammatory cell infiltration. In the case of the connective tissues, the endoneurium were broken, perineurium displayed partial impairment, but epineurium remained intact.

4. Discussion

Currently, as the sciatic nerve crush model does not require introduction of microsurgical techniques and avoids the strict requirements for nerve suture, it therefore has been one of the most commonly used experimental models for PNI [21,22]. In this model, as the continuity of axons is disrupted while the corresponding connective tissue and the Schwann cell basal lamina are not impaired, the continuity of the nerve trunk maintained, and it provides an optimal pathway for the regeneration of broken axons [23,24]. More recently, some investigators have explored the standardization of assessment methods of the PNI using devices such as a non-serrated clamp for induction of a sciatic nerve clamp injury model, thus confirming the advantages of repeatability and homogeneity in the sciatic nerve clamp injury model [25–29]. Nevertheless, in terms of the assessment on the model, we were also unable to prove whether the model was successful due to the lack of exact evaluation indicators. For this reason, we attempted to find appropriate methods to achieve a more precisely assessment of the rat sciatic nerve crush injury model by using CMAP and behavioral and morphological methods.
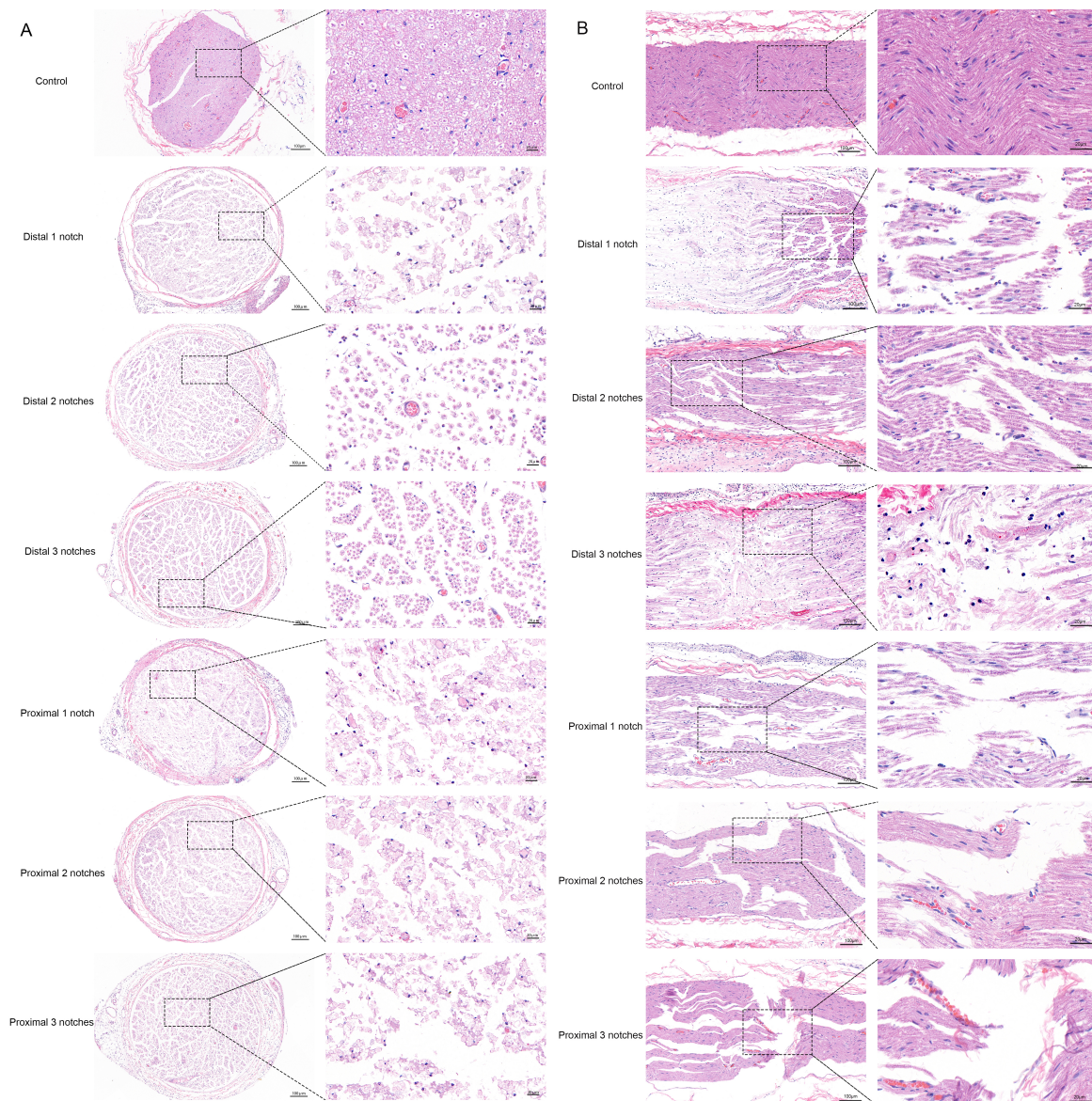
Fig. 5. H&E staining of the sciatic nerve. (A) H&E staining of the sciatic nerve cross sections of rats. (B) H&E staining of the sciatic nerve longitudinal sections of rats.

Electrophysiological examination provides an objective approach to nerve function assessment [30]. Signal latency reflects the time necessary for the fast conducting motor fibers to reach the muscle and a prolonged latency indicates that the nerve has developed a demyelinating lesion; Amplitude reflects the number of muscle fibers contributing to a compound neuromuscular action potential and axonal injury results in a marked decrease in the amplitude of this action potential. Relevant studies have shown that the amplitude was considered to indicate a nerve conduction block when it was decreased by more than 50% [31]; In previous studies, it was generally believed that if the amplitude decreased to 0 mV, induction of the sciatic nerve crush injury model was successful [32]. NCV mainly reflects pathophysiological states of fast and crude fibers in nerve trunk. As a general rule, the NCV was considered

abnormal at a value of $\leq 20\%$, and that both demyelinating lesions and severe axonal injury significantly slow an NCV. In the results presented here, conduction studies in the distal three notches group revealed a significantly longer latency and marked decrease of the amplitude and NCV. There was almost no conduction of impulses from the onset of the distal two notches group. Excluding the occasional detection within the distal two notches group (almost 0), no amplitude was detected in other more seriously injured groups. Additionally, the CMAP latency and NCV were undetectable starting at force values similar to those of the distal two notches group.

In animal experiments, SFI is a classical indicator of motor function and has been widely used to research nerve function after PNI [33]. Motor function on the injured side was obviously limited in the sciatic nerve clamp injury

model. It was not surprising that the rats experienced claudication on the day of modeling, given that these rats suffered pain during the acute phase of sciatic nerve crush injury. This indicated temporary complete loss of motor function. From the SFI measurement results at day three after modeling, walking ability became progressively weaker as the force values obtained from the forceps increased during modeling. Motor function was lost entirely when the pressure increased to approximately the distal one notch pressure and the affected limb either dragged on the ground or was completely off the ground.

PWT and PWL were the main ethological indices employed to quantitatively evaluate recovery of sensory function. They were both significantly decreased among all groups of rats following sciatic nerve injury. Among them, the most apparent and the and least severe model corresponded to the proximal three notches group and the distal one notch group, respectively. Aside from this, the distal and proximal one notch groups and were relatively heavy and the magnitude of both injuries were comparable, indicating that PWT and PWL exhibited a decreased trend with increasing crush pressures, while the effects of crush injury on PWT and PWL were obvious from the distal one notch group.

Sunderland Classification of Nerve Injuries is a classical method which divides nerve injury into five different levels of damage according to pathological manifestations and features of different impairments [34]. In this study, the distal three notches group presented with minor nerve injuries, intact axons and sheaths, phased demyelinated alterations, but without axon degeneration or temporary loss of conduction function. All of these characteristics were consistent with a Sunderland grade I injury (Neurapraxia) which spontaneously resolved after a few days. The distal two notches group had the characteristics necessary for a Sunderland grade II injury, such as axon disruptions, endoneurium intact and Wallerian degeneration in the injured distal segments. Although such lesions were more serious, the proximally regenerated axons grew to the terminal organ along the distal nerve endoneurium tube and were still self-recovered. Axons, myelin and endoneurium were damaged in distal one, proximal one and proximal two notch groups. In the distal and proximal one notch groups, endoneurium showed partial damage, and proximal two notches group was fully broken, while perineurium and epineurium were still intact. These groups all belong to Sunderland grade III injury and fail to completely recover by themselves and it is widely used in short-term functional repair after PNI [35]. The most severe injuries were acquired in the proximal three notches group. The nerve axon, myelin sheath and endoneurium were broken and perineurium partially ruptured, but the epineurium remained intact in the damaged nerve, which conforms to the characteristics of a Sunderland grade III–IV injury. The nerve trunk was completely broken and exhibits loss of continuity in a Sunderland grade V injury, which was one that could not be achieved with the clamp injury model. Sunderland grades IV and V are not easily recovered from and require surgical intervention.

It is not surprising to find that the accuracy of electrophysiological examinations was further confirmed by morphological results of each group. Ultrastructurally, the sciatic nerve of rats in the distal three notch group showed segmental demyelination, which was characterized by the destruction of the myelin sheath while the axonal structures remained intact. Consequently, the nerve conduction was still present despite alterations in the CMAP. Distinct from this, in the distal two group, both axon and surrounding myelin break down was apparent, axonal continuity was lost and conduction of impulses was no longer possible from the onset of the distal two group. Undoubtedly, there was also no nerve conduction in the more serious nerve damage groups (see more details in Table 1). We thus argue that the degree of nerve injury directly affects nerve conduction function. The CMAP in crushed peripheral nerves are closely related to the severity of the initial injury. As a result, in contrast to other evaluation methods, electrophysiological examinations are more sensitive indicators of nerve damage in the early stage of the sciatic nerve crush model. We could able to detect and quantify neuropathy severity by neuroelectrophysiological examinations.

5. Conclusions

The results clearly show that, among all evaluation methods, neuroelectrophysiological examination is more accurate in identification of the degree of nerve damage. We believe that it is more instructive to consider the changes in electrophysiological tests in conjunction with the changes in morphological characteristics for the sciatic crush injury model. These methods may overcome the problem that the degree of damage implemented in the model was otherwise difficult to accurately evaluate, so as to greatly increase the objectivity of the experiment, thus providing a simple, easy, reproducible, standardized approach to sciatic crush injury modelling.

Abbreviations

PNI, peripheral nerve injury; CMAP, compound muscle action potential; MNCV, motor nerve conduction velocity; SFI, sciatic functional index; PWT, paw withdrawal threshold; PWL, paw withdrawal latency.

Author contributions

YA, HXY, JNZ conducted the experiments and wrote the manuscript, XMY conducted the data analysis, JTY designed the present research.

Ethics approval and consent to participate

Acknowledgment

Funding

Conflict of interest

The authors declare no conflict of interest.

References

[1] Huang J, Zhang Y, Lu L, Hu X, Luo Z. Electrical stimulation accelerates nerve regeneration and functional recovery in delayed peripheral nerve injury in rats. The European Journal of Neuroscience. 2013; 38: 3691–3701.

[2] Xing L, Cheng Q, Zha G, Yi S. Transcriptional Profiling at High Temporal Resolution Reveals Robust Immune/Inflammatory Responses during Rat Sciatic Nerve Recovery. Mediators of Inflammation. 2017; 2017: 3827841.

[3] Ma F, Xiao Z, Meng D, Hou X, Zhu J, Dai J, et al. Use of natural neural scaffolds consisting of engineered vascular endothelial growth factor immobilized on ordered collagen fibers filled in a collagen tube for peripheral nerve regeneration in rats. International Journal of Molecular Sciences. 2014; 15: 18593–18609.

[4] Wang M, Theis T, Kabat M, Loers G, Agre LA, Schachner M. Functions of Small Organic Compounds that Mimic the HNK-1 Glycan. International Journal of Molecular Sciences. 2020; 21: 7018.

[5] Campbell WW. Evaluation and management of peripheral nerve injury. Clinical Neurophysiology. 2008; 119: 1951–1965.

[6] Geuna S, Raimondo S, Ronchi G, Di Scipio F, Tos P, Czaja K, et al. Chapter 3: Histology of the Peripheral Nerve and Changes Occurring during Nerve Regeneration. International Review of Neurobiology. 2009; 32: 27–46.

[7] Geuna S. The sciatic nerve injury model in pre-clinical research. Journal of Neuroscience Methods. 2015; 243: 39–46.

[8] Heinzel JC, Oberhauser V, Keibl C, Swiadek N, Längle G, Frick H, et al. Evaluation of Functional Recovery in Rats After Median Nerve Resection and Autograft Repair Using Computerized Gait Analysis. Frontiers in Neuroscience. 2021; 14: 593545.

[9] Renno WM, Afzal M, Paul B, Nair D, Kumar J, Al-Hassan JM. Catfish Epidermal Preparation Accelerates Healing of Damaged Nerve in a Sciatic Nerve Crush Injury Rat Model. Frontiers in Pharmacology. 2021; 12: 632028.

[10] Varejão ASP, Cabrita AM, Meek MF, Bulas-Cruz J, Melo-Pinto P, Raimondo S, et al. Functional and morphological assessment of a standardized rat sciatic nerve crush injury with a non-serrated clamp. Journal of Neurotrauma. 2004; 21: 1652–1670.

[11] Luís AL, Amado S, Geuna S, Rodrigues JM, Simões MJ, Santos JD, et al. Long-term functional and morphological assessment of a standardized rat sciatic nerve crush injury with a non-serrated clamp. Journal of Neuroscience Methods. 2007; 163: 92–104.

[12] Renno WM, Al-Maghrebi M, Rao MS, Khraishah H. (-)-Epigallocatechin-3-gallate modulates spinal cord neuronal degeneration by enhancing growth-associated protein 43, B-cell lymphoma 2, and decreasing B-cell lymphoma 2-associated x protein expression after sciatic nerve crush injury. Journal of Neurotrauma. 2015; 32: 170–184.

[13] Renno WM, Khan KM, Benov L. Is there a role for neurotrophic factors and their receptors in augmenting the neuroprotective effect of (-)-epigallocatechin-3-gallate treatment of sciatic nerve crush injury? Neuropharmacology. 2016; 102: 1–20.

[14] Renno WM, Al-Maghrebi M, Alshammari A, George P. (-)-Epigallocatechin-3-gallate (EGCG) attenuates peripheral nerve degeneration in rat sciatic nerve crush injury. Neurochemistry International. 2013; 62: 221–231.

[15] de Medinaceli L, Freed WJ, Wyatt RJ. An index of the functional condition of rat sciatic nerve based on measurements made from walking tracks. Experimental Neurology. 1982; 77: 634–643.

[16] Syu W, Hueng D, Chen W, Chan JY, Chen S, Huang S. Adipose-Derived Neural Stem Cells Combined with Acellular Dermal Matrix as a Neural Conduit Enhances Peripheral Nerve Repair. Cell Transplantation. 2019; 28: 1220–1230.

[17] Dixon WJ. Efficient analysis of experimental observations. Annual Review of Pharmacology and Toxicology. 1980; 20: 441–462.

[18] Chaplan SR, Bach FW, Pogrel JW, Chung JM, Yaksh TL. Quantitative assessment of tactile allodynia in the rat paw. Journal of Neuroscience Methods. 1994; 53: 55–63.

[19] Hargreaves K, Dubner R, Brown F, Flores C, Joris J. A new and sensitive method for measuring thermal nociception in cutaneous hyperalgesia. Pain. 1988; 32: 77–88.

[20] Yang H, Wu L, Deng H, Chen Y, Zhou H, Liu M, et al. Anti-inflammatory protein TSG-6 secreted by bone marrow mesenchymal stem cells attenuates neuropathic pain by inhibiting the TLR2/MyD88/NF-κB signaling pathway in spinal microglia. Journal of Neuroinflammation. 2020; 17: 154.

[21] Bridge PM, Ball DJ, Mackinnon SE, Nakao Y, Brandt K, Hunter DA, et al. Nerve crush injuries–a model for axonotmesis. Experimental Neurology. 1994; 127: 284–290.

[22] Savastano LE, Laurito SR, Fitt MR, Rasmussen JA, Gonzalez Polo V, Patterson SI. Sciatic nerve injury: a simple and subtle model for investigating many aspects of nervous system damage and recovery. Journal of Neuroscience Methods. 2014; 227: 166–180.

[23] Burian E, Sollmann N, Ritschl LM, Palla B, Maier L, Zimmer C, et al. High resolution MRI for quantitative assessment of inferior alveolar nerve impairment in course of mandible fractures: an imaging feasibility study. Scientific Reports. 2020; 10: 11566.

[24] Massaad CA, Zhang G, Pillai L, Azhdarinia A, Liu W, Sheikh KA. Fluorescently-tagged anti-ganglioside antibody selectively identifies peripheral nerve in living animals. Scientific Reports. 2015; 5: 15766.

[25] Beer GM, Steurer J, Meyer VE. Standardizing nerve crushes with a non-serrated clamp. Journal of Reconstructive Microsurgery. 2001; 17: 531–534.

[26] Varejão ASP, Cabrita AM, Meek MF, Bulas-Cruz J, Melo-Pinto P, Raimondo S, et al. Functional and morphological assessment of a standardized rat sciatic nerve crush injury with a non-serrated clamp. Journal of Neurotrauma. 2004; 21: 1652–1670.

[27] Chen LE, Seaber AV, Urbaniak JR. The influence of magnitude and duration of crush load on functional recovery of the pe-

ripheral nerve. Journal of Reconstructive Microsurgery. 1993; 9: 299–306.

[28] Chen LE, Seaber AV, Glisson RR, Davies H, Murrell GA, Anthony DC, *et al*. The functional recovery of peripheral nerves following defined acute crush injuries. Journal of Orthopaedic Research. 1992; 10: 657–664.

[29] Wright MC, Mi R, Connor E, Reed N, Vyas A, Alspalter M, *et al*. Novel roles for osteopontin and clusterin in peripheral motor and sensory axon regeneration. The Journal of Neuroscience. 2014; 34: 1689–1700.

[30] Choi JM, Di Maria G. Electrodiagnostic Testing for Disorders of Peripheral Nerves. Clinics in Geriatric Medicine. 2021; 37: 209–221.

[31] Gerber D, Ghidinelli M, Tinelli E, Somandin C, Gerber J, Pereira JA, *et al*. Schwann cells, but not Oligodendrocytes, Depend Strictly on Dynamin 2 Function. eLife. 2019; 8: e42404.

[32] Wang Z, Qin L, Zhang W, Zhang P, Jiang B. Qian-Zheng-San promotes regeneration after sciatic nerve crush injury in rats. Neural Regeneration Research. 2019; 14: 683–691.

[33] de Medinaceli L, Freed WJ, Wyatt RJ. An index of the functional condition of rat sciatic nerve based on measurements made from walking tracks. Experimental Neurology. 1982; 77: 634–643.

[34] Sunderland S. A classification of peripheral nerve injuries producing loss of function. Brain. 1951; 74: 491–516.

[35] Grinsell D, Keating CP. Peripheral Nerve Reconstruction after Injury: a Review of Clinical and Experimental Therapies. BioMed Research International. 2014; 2014: 698256.